Application of Swept-Sine Excitation for Acoustic Impedance Eduction

Brian M. Howerton[1]
NASA Langley Research Center, Hampton, VA, 23681

Håvard Vold[2]
Vold LLC, Charleston, SC 29412

Michael G. Jones[3]
NASA Langley Research Center, Hampton, VA, 23681

The NASA Langley Normal Incidence Tube (NIT) and Grazing Flow Impedance Tube (GFIT) are regularly employed to characterize the frequency response of acoustic liners through the eduction of their specific acoustic impedance. Both test rigs typically use an acoustic source that produces sine wave signals at discrete frequencies (Stepped-Sine) to educe the impedance. The current work details a novel approach using frequency-swept sine waveforms normalized to a constant sound pressure level for excitation. Determination of the sound pressure level and phase from microphone measurements acquired using swept-sine excitation is performed using a modified Vold-Kalman order tracking filter. Four acoustic liners are evaluated in the NIT and GFIT with both stepped-sine and swept-sine sources. Using these two methods, the educed impedance spectra are shown to compare favorably. However, the new (Swept-Sine) approach provides much greater frequency resolution in less time, allowing the acoustic liner properties to be studied in much greater detail.

I. Introduction

Acoustic liners have been successfully applied to reduce the radiated noise created by turbofan engines in order to meet ever more stringent noise constraints. Research efforts by NASA and others have focused mostly on understanding liner physics and how to optimize their impedance for the greatest noise reduction. Determination of the complex impedance of materials and structures used in noise control applications is the primary measurement required to understand the acoustic performance of these absorbers. Since impedance is an intrinsic property of the material, it should also be invariant with the means by which it is educed. The value of this complex quantity for duct acoustics lies in its ability to be applied to other duct geometries whereas measurements of attenuation or insertion loss are specific to the duct in which they were acquired.

Many methods can be used to determine acoustic impedance for both normal and grazing sound incidence. Dickens et al. [1] describe the merits and detractions of various schemes using a waveguide and traditional microphone measurements as well as combinations of alternative instrumentation. There is also discussion on calibration effects and source signal optimization showing them to be important in maximizing the accuracy of the result. Direct, *in situ* measurements as described by Dean [2] allow for determination of impedance using simple microphone measurements placed in the liner but can be prone to errors if the sensor locations are not chosen judiciously. Further work by Gaeta et al. [3] applied Dean's method to a normal incidence impedance tube as well as grazing flow impedance tubes at

[1] Research Scientist, Structural Acoustics Branch, Senior Member AIAA, (brian.m.howerton@nasa.gov).
[2] Founder, Associate Fellow AIAA, (hvold@vold.com).
[3] Senior Research Scientist, Structural Acoustics Branch, Associate Fellow AIAA.

NASA Langley and Georgia Tech with reasonable accuracy. Research by Jones and Stiede [4] at NASA Langley, using the Normal Incidence Tube (NIT), evaluated several processing techniques and acoustic sources for determining impedance with rankings by accuracy and measurement time. Results showed the Switching Two-Microphone Method (using discrete tones) coupled with a multipoint analysis provided the best compromise. This method has become the preferred technique for impedance eduction with the NIT.

The choice of acoustic sound source carries with it some tradeoffs and compromises to balance speed and accuracy. Discrete tones (referred to here as Stepped-Sine) can be used as a source excitation to march through the frequency domain at some interval while acquiring the acoustic pressures necessary for impedance eduction. There is a time penalty required to do these measurements if the frequency interval is small. Generally, 100 to 200 Hz intervals are used, which may not be sufficient to properly resolve all the features of the impedance spectra especially for more exotic multidegree-of-freedom liners that are of interest to the liner community [5,6]. Excitation using random noise (typically white noise) has the advantage of containing acoustic energy over a wide range of frequencies when paired with the appropriate driver. This allows for measurement and calculation of specific acoustic impedance across all frequencies simultaneously. One disadvantage is the resultant variation in the pressure spectrum at the sample face due to an inability to hold the target amplitude constant over the full frequency range. Accuracy can suffer when testing nonlinear liners in this manner. Pseudorandom and multitone sources where multiple frequencies are generated simultaneously offer a potential solution to surface pressure spectrum variation with appropriate feedback and iteration of the source signal. Acquisition time can be reduced significantly if an efficient procedure is employed to create a normalized source signal with the desired SPL. However, it has been shown by Bodén [7,8] that the measured impedance spectra acquired with multifrequency excitation can differ from that acquired using single tones. The sample reacts to all frequencies to which it is exposed, which can alter the acoustic particle velocity at any particular frequency especially for higher amplitudes.

Use of swept-sine excitation has been employed in structural, material and electrical engineering testing to determine the response of a given system whether it be linear or nonlinear. The current investigation is focused on evaluating the use of swept-sine acoustic excitation in conjunction with order tracking filters to acquire the necessary data for impedance eduction. Such excitation can allow for rapid acquisition of accurate acoustic pressure data while avoiding the issues with multitone and random noise sources. This method has been applied to the acquisition systems of the NIT and GFIT at Mach 0.0. Four acoustic liners were tested in each rig using traditional stepped-sine as well as a swept-sine excitation in order to compare the educed impedances from each. The intent of using a swept-sine excitation is to provide greater frequency content in the impedance spectra with an equivalent, or even reduced, acquisition time relative to the Stepped-Sine method.

II. Swept-Sine Method

The Swept-Sine Method (SSM) attempts to obtain the complex acoustic cross spectra between the measurement microphones and the source signal supplied to the acoustic drivers. The method offers fine frequency resolution and reduced data acquisition time by sweeping sinusoidal excitation continuously across the frequency range instead of dwelling on discrete frequencies as in the Stepped-Sine process. The resulting spectra are used to educe the acoustic impedance of the liner.

A. The Wold decomposition of a stochastic process

In the late 1930s, Herman Wold, a Norwegian-Swedish mathematician, formulated the first versions of what would become known as the *Wold decomposition*. The decomposition states that any stationary stochastic process can be broken into the uncorrelated sum of a *purely deterministic* process and a *purely indeterministic* process [9]. The deterministic process could be regarded as a sum of sine waves with various phases and amplitudes, and the purely indeterministic component could be represented as a white noise process filtered by an (infinite) moving average filter. The sine waves would have point spectra with finite spectral mass at discrete frequencies, while the purely indeterministic component would have an absolutely continuous spectral density, corresponding to a broadband noise process. The total measured signal y(t), encompassing the sum of deterministic and indeterministic components is of the form:

$$y(t) = x(t) + v(t) \tag{1}$$

where $x(t)$ is the deterministic periodic response and $v(t)$ is causal and uncorrelated with $x(t)$, and has an absolutely continuous spectrum without tonal content. The signal $v(t)$ is thereby the purely indeterministic component of the Wold decomposition.

B. The anatomy of sinusoidal excitation and response

Stationary periodic excitation of a nonlinear system will cause a stationary response of the same period. The Fourier theorem states that a periodic function may be expressed as a sum of sinusoids or harmonics, each with a frequency that is an integral multiple of a base frequency. These sinusoids will have their own amplitude and phase. In the swept-sine testing, the excitation frequency is constantly changing (whether linearly or exponentially). Thus, the total system response will be a sum of the steady state response of the system to the swept excitation and any transients.

The instantaneous frequency of oscillation in revolutions per second can be denoted as $\omega(t)$. The instantaneous rotational angle is the time integral of the frequency, and the complex phasor $p_{k(t)}$ belonging to the order (or harmonic) k is defined as:

$$p_k(t) = exp(2\pi ik \int_0^t \omega(u)du). \tag{2}$$

The order *k* does not have to be an integer; in machinery, toothed gears give rise to rational orders, and rolling element bearings and pulleys most often produce irrational orders. A complex order time history, $x_k(t)$, can be defined as:

$$x_k(t) = A_k(t)p_k(t) = A_k(t)\exp(2\pi ik \int_0^t \omega(u)du) \tag{3}$$

where $A_k(t)$ is a slowly varying complex envelope. This allows the general case of a vibration or acoustic time history resulting from a periodic excitation to be expressed as:

$$x(t) = \sum_{s\in S}\sum_{k\in\mathcal{K}_s} A_{sk}(t)p_{sk}(t) = \sum_{s\in S}\sum_{k\in\mathcal{K}_s} A_{sk}(t)\exp(2\pi ik \int_0^t \omega_s(u)\,du) \tag{4}$$

where S is the set of all independent, periodic sources, and $\mathcal{K}_S$ is the set of all orders, negative as well as positive, generated by source *s*.

Since Eq. (4) is a sum of sine waves, this time history is a completely deterministic process in the language of the Wold decomposition [9]. Because of this property, each order, when observed synchronously with multiple sensors, is fully self-coherent, which makes is feasible to construct spatial mappings of each order as a function of time, rpm or frequency [10]. In the current application, when measuring the acoustic responses from periodically excited systems, the effects of flow noise, turbulence and transient events are also recorded as the indeterministic component, $v(t)$, signal from Eq. (1).

C. The Vold-Kalman filter

One can assume that a digitized, finite, alias-free response time history exists, denoted as $y(n); n \in [0,1,\dots,N]$ where the sampling rate has been set to one sample per second without any loss of generality. Also, frequencies $\omega_s(n)$ for the periodic sources $s \in S$ are known. Order tracking is the art and science of estimating the complex envelopes $A_{sk}(n)$ from the recorded response and excitation frequencies for the orders $\in \mathcal{K}_s$, restricted to the orders of lower frequency than the Nyquist frequency of 0.5 Hz. These complex envelopes are estimated using a Vold-Kalman filter applied to the measured time history data. The Vold-Kalman filter [11] is related to the classical Kalman filter [12] by compromising between structural equations and data equations, although in the Vold-Kalman filter, one only uses the ratio between the two sets of equations. The *structural equation* specifies that the envelope functions should be smooth, slowly varying functions. One way of specifying this for the envelope $A_{sk}(n)$, is to demand that a repeated difference should be small, e.g., satisfy one of the following equations:

$$\begin{aligned} \nabla A_{sk}(n) &= A_{sk}(n+1) - A_{sk}(n) &&= \epsilon(n) \\ \nabla^2 A_{sk}(n) &= A_{sk}(n+2) - 2A_{sk}(n+1) - A_{sk}(n) &&= \epsilon(n) \\ \nabla^3 A_{sk}(n) &= A_{sk}(n+3) - 3A_{sk}(n+2) + 3A_{sk}(n+1) - A_{sk}(n) &&= \epsilon(n) \end{aligned} \tag{5,6,7}$$

where the sequence $\epsilon(n)$ is small in some sense. The exponent q in the difference operator ∇^q is customarily named the *pole count* of the Vold-Kalman filter. The coefficients of the expanded iterated differences are seen to build the famous *Pascal triangle*.

In addition to the smoothness condition of the structural equation, the estimated complex envelope function must somehow be related to the measured data, and this is achieved by the *data equation*:

$$\sum_{s\in S}\sum_{k\in\mathcal{K}_s} A_{sk}(n)p_{sk}(n) - y(n) = \nu(n) \tag{8}$$

which is seen to be a reordered discrete version of Eqs. (1,4).

The unknown complex envelope functions $A_{sk}(n)$ occur in linear expressions with measured coefficients on the left hand side of the structural and data equations. A weighted linear least squares problem can be constructed by choosing a weighting function $r(n)$; $n \in [0,1,\dots,N]$, and discarding the unmeasured functions $\epsilon(n)$ and $\nu(n)$ as nuisance parameters to obtain the linear, overdetermined set of equations:

$$r(n)\nabla^q A_{sk}(n) \approx 0$$

$$\sum_{s\in S}\sum_{k\in\mathcal{K}_s} A_{sk}(n)p_{sk}(n) \approx y(n) \tag{9,10}$$

where a large value of $r(n)$ enforces smoothness around the time point *n*, while a small value permits the observed data to dominate the estimation at this time point. The choice of the weighting function $r(n)$ determines the bandwidth and the resolution of the results [12].

D. Simple solution for single-source, swept-sine excitation

A substantial reduction in computation and storage is possible for the case of a single excitation source. The basic idea may be found by considering a single order *k* to be extracted with a corresponding weighting function $r(n)$ and the phasor:

$$p_k(n) = \exp(2\pi i k \sum_{l=0}^{n} \omega(l)) . \tag{11}$$

The overdetermined Eqs. (9,10) simplify to:

$$\begin{aligned} r(n)\nabla^q A_k(n) &\approx 0 \\ p_k(n)A_k(n) &\approx y(n) \end{aligned} \tag{12,13}$$

where Eq. (13) may be rewritten as:

$$1A_k(n) \approx {p_k}^{-1}(n)y(n) \tag{14}$$

whereby it is seen that the left hand side becomes that of a phasor of constant frequency zero, and a *time variant zoom* transformation on the right hand side. The coefficient matrix is then of length $N+1$, and semi-bandwidth $q+1$. The inverses of the phasor functions may always be applied, since the absolute value of any phasor is always 1. The weighting function corresponding to a bandwidth function $h(n)$ with a 3dB rolloff is given by:

$$r(n) = \sqrt{\frac{\sqrt{2}-1}{(2(1-\cos(2\pi h(n))))^q}} . \tag{15}$$

The bandwidth is either chosen to be constant or proportional to the frequency of excitation. This expression was first derived by Tuma [13]. In the impedance eduction application, only the first order is to be extracted, and the pole count q is normally chosen to be two, in which case the overdetermined Eqs. (12,13) may be written in matrix form as:

$$\begin{Bmatrix} R\,\triangle \\ I \end{Bmatrix} A_1 \approx \begin{bmatrix} 0 \\ p_1^{-1} y \end{bmatrix} \tag{16}$$

where R is the diagonal matrix formed by the elements of the weighting coefficients $r(n)$, A_1 is the column vector of the complex $A_1(n)$ and Δ is the banded matrix of the iterated difference coefficients:

$$\Delta = \begin{bmatrix} 1 & -2 & 1 & \dots & \dots \\ \dots & 1 & -2 & 1 & \dots \\ \dots & & & & \end{bmatrix} \tag{17}$$

The usual least squares solution by normal equations is found by premultiplying Eq. (16) by the transpose of the coefficient matrix and using the *Cholesky decomposition* to solve the banded *positive definite real* set of equations:

$$(\Delta^H R^2 \Delta + I) A_1 = p_1^{-1} y. \tag{18}$$

The coefficient matrix is constant for all response measurements and needs to be decomposed only once. The right hand side of Eq. (18) is complex.

E. Calculating the excitation signal

The excitation signal is a numerical and mathematical entity generated by the computer and then output to analog devices through digital-to-analog converters and amplifiers. As it is being output, phase-synchronized digital recording of electrical and acoustic responses takes place, such that one can obtain highly reliable deterministic relationships between input and output. In this section, discrete time is assumed since both the excitation signal and the responses are recorded in the digital domain.

1. Structure of the excitation signal

The excitation signal is normally a monotonically nondecreasing sweep in frequency to cover each frequency region in sufficient detail to extract good estimates of the relationships between excitation and response. In frequency ranges where issues pertaining to noise or nonlinearities occur, a longer dwell time can be used to allow for statistical averaging and decay of transients. When the transients decay, the sweep will only contain one frequency at any given instant of time, so that the excitation signal can be described as the real part of the expression:

$$z(n) = \mathrm{Re}\left(Z(n) \exp(2\pi i \int_0^{ndt} \omega(u) du \right) \tag{19}$$

where $Z(n)$ is the complex envelope of the excitation at time n.

2. Computing cross spectra

Since the excitation at time n only has energy at the frequency $\omega(n)$, the responses may have energy at harmonics of the frequency, but when considering spectra and cross spectra, the complex amplitudes of the measured signals at the fundamental frequency need only be extracted using the Vold-Kalman filter. Consider two sensors **A** and **B**, and denote their complex amplitudes as extracted with the Vold-Kalman filter at time n as $A(n)$ and $B(n)$. Since the excitation frequency is $\omega(n)$, the cross spectrum estimate is:

$$G_{AB}\big(\omega(n)\big) = A(n)\bar{B}(n) \tag{20}$$

Since the estimates are obtained at the sampling rate, averaging estimates over $2p$ time steps can be used to reduce the variance of the cross spectral estimate at time n by the expression:

$$G_{AB}(\omega(n), p) = \frac{1}{2p+1} \sum_{k=-p}^{p} A(n+k)\bar{B}\,(n+k). \tag{21}$$

This average will be less sensitive to random and transient effects and be more true to the underlying deterministic response.

3. Tuning for a flat response at the reference microphone

The impedance of a liner may depend on the excitation level. Thus, it is generally educed from measurements where the power at a reference microphone is held constant versus frequency. To obtain a consistent excitation signal level versus frequency, one must compute a frequency-dependent gain adjustment based on response data collected during a constant amplitude, preliminary run. The response may then be analyzed to account for nonlinearity in the source generation hardware and the influence of the liner sample. If the reference microphone channel is denoted by A and the excitation channel by Z, after the first run with a given excitation signal, an estimate of the transfer function (dropping the time point n from the notation) is:

$$H = \frac{G_{AZ}}{G_{ZZ}} \tag{22}$$

Now, if the response is A, and should have been $A(1+\alpha)$, a suitable linearized correction δ to the excitation is found by solving:

$$A(1+\alpha) = HZ(1+\delta) \Rightarrow \delta = {}^{A\alpha}/_{H} \tag{23}$$

Note that the correction is frequency dependent, even though the time and frequency dependence in notation is dropped in this section. Experience with the simple linearized correction factor showed that, while the corrections mostly converge quickly, nonlinear responses of the liner may result in instability and nonconvergence of reference microphone levels. This behavior is averted by multiplying the correction δ with scalar gain factor $0 < k <= 1.0$, which has demonstrated convergence to a flat response level within a few iterations for a k value of 0.8. Further optimization *could* be achieved by making the correction and gain factors frequency dependent to account for this nonlinear behavior but would require *a priori* knowledge of the liner response. Another approach is to store a sample's optimized sweep to use as the starting point for the next sample. If the difference in sample impedances are minor, normalization of the excitation signal should be rapid.

Since the excitation signal is externally generated, it must be incoherent with the self noise at any response location. Thus, when an estimate of the cross spectrum between two sensors **A** and **B** is desired**,** one can use the estimator:

$$\tilde{G}_{AB} = \frac{G_{AZ}G_{ZB}}{G_{ZZ}} \tag{24}$$

as the sensor self noise must be incoherent with the excitation.

III. Experiment

The experimental investigation involves testing of four acoustic liner configurations in the NIT and GFIT with stepped-sine and swept-sine acoustic excitation. The liners were chosen to provide a range of educed impedances and spectral features. Configurations GE01 and GE03 are conventional perforate over honeycomb with differing facesheet hole size and porosity. The impedance spectra of GE01 and GE03 should be nonlinear with SPL. A ceramic tubular liner (CT57) is included to provide a control sample to evaluate the impedance eduction results. Its narrow, parallel tube geometry is ideal for study as the impedance can be predicted from first principles and it acoustic response is linear. A 3-D printed version of the tubular liner was developed using Stereolithography (SLA). This sample (CSQ3) is comprised of an array of narrow, parallel square chambers. The porosity is lower than the CT57 sample but higher than GE01 and GE03. In all cases, samples are terminated with a rigid backplane. The sample dimensions are provided in Table 1.

Table 1. Liner sample parameters.

	Liner Sample			
Parameter	**CT57**	**GE01**	**GE03**	**CSQ3**
POA	57	8.7	15	22
Perforate dim. (mm)	0.635 (dia.)	1 (dia.)	1 (dia.)	1.27 x 1.27
Facesheet Thickness (mm)	N/A	0.635	0.635	N/A
Sample Thickness (mm)	50.8/80.7 (NIT/GFIT)	38.1	38.1	76.2

A. Liner Samples (NIT)

For this study, the liner geometries consist of 50.8mm x 50.8mm samples surrounded by a 6.35mm thick wall. The active area of the sample matches the cross-sectional area of the NIT waveguide. Figure 1 shows a photo of the four samples to illustrate differences in their surface features.

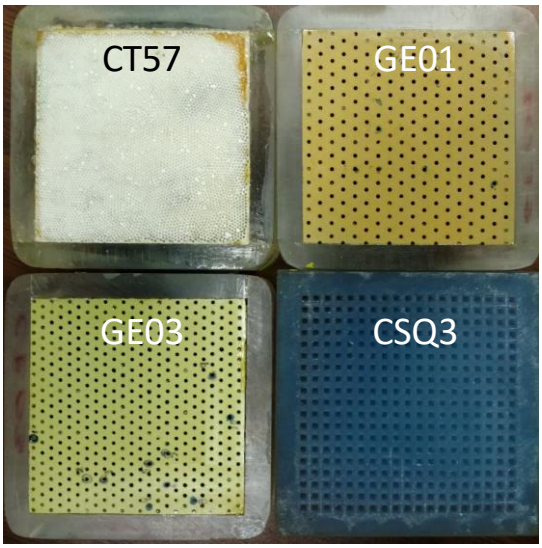

Fig. 1 NIT liner samples.

B. Liner Samples (GFIT)

The samples tested in the GFIT are of the same construction as the NIT samples but of larger dimension. Width of the sample active area is retained at 50.8 mm, but the length increases to, nominally, 415 mm. All configurations are terminated with a rigid backplate. Figure 2 is a photograph of the liner samples.

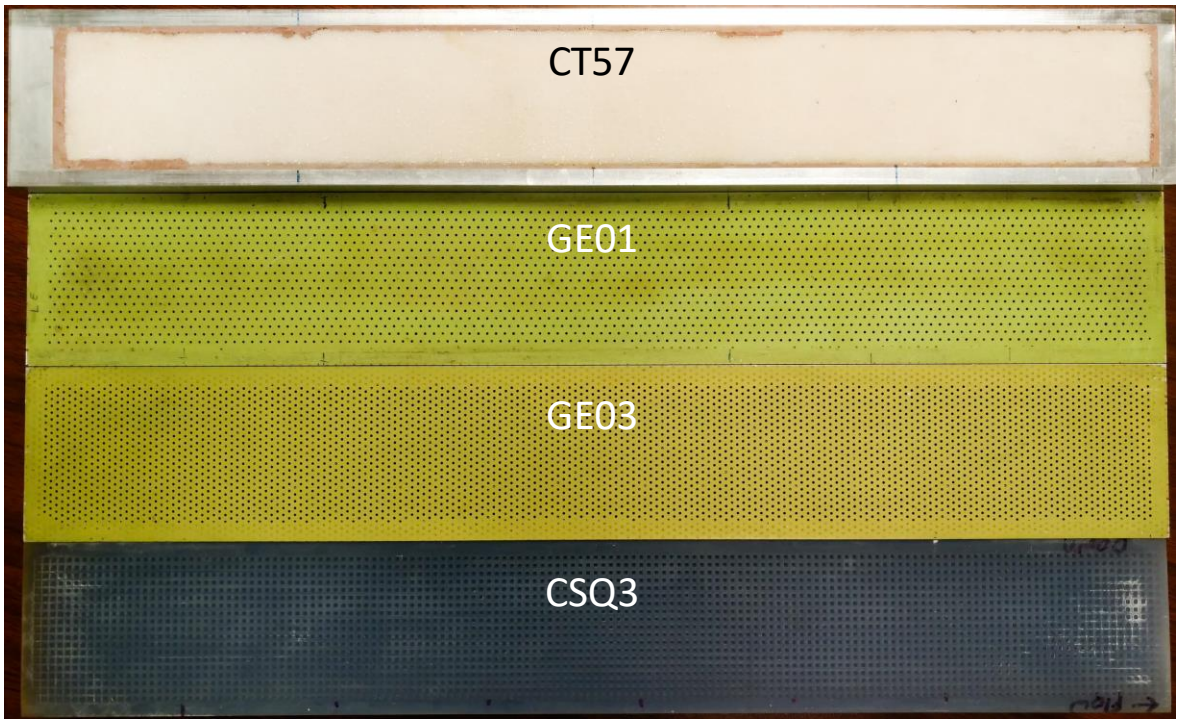

Fig. 2 GFIT liner samples.

C. Normal Incidence Tube (NIT)

The NIT consists of a group of six electromagnetic acoustic drivers coupled radially into a cylindrical tube that transitions to the 50.8 mm x 50.8 mm (2 in x 2 in) square cross-section waveguide. Samples are placed at the exit of the tube to be exposed to the generated sound field. Individual digital-to-analog converters for each speaker allow for the creation of arbitrary waveforms to energize each driver. Typically, tonal or broadband signals are employed for impedance eduction. For tones, levels of 150 dB can be consistently achieved while broadband is limited to an OASPL of 140 dB across the typical measurement range of frequencies (400 to 3000 Hz). Impedance spectra for each sample are obtained in the NIT via the Two-Microphone Method (TMM) [4]. The key feature of the TMM is the efficient acquisition of the complex transfer function spectra between two flush-mounted microphones strategically located in the standing wave field from which the complex reflection factor is calculated. Transfer function accuracy is assured by a microphone switching technique that avoids labor intensive amplitude and phase calibrations. Several operational features have also been incorporated to maximize test efficiency. The microphone switching is automated by means of a computer-controlled stepping motor that rotates the microphone holder while a feedback loop and iterative scheme is used to adjust sound pressure levels to the desired value. Custom software controls all aspects of the acquisition and reporting process and can step through a test matrix without user intervention. Figure 3 shows the general arrangement of the NIT apparatus.

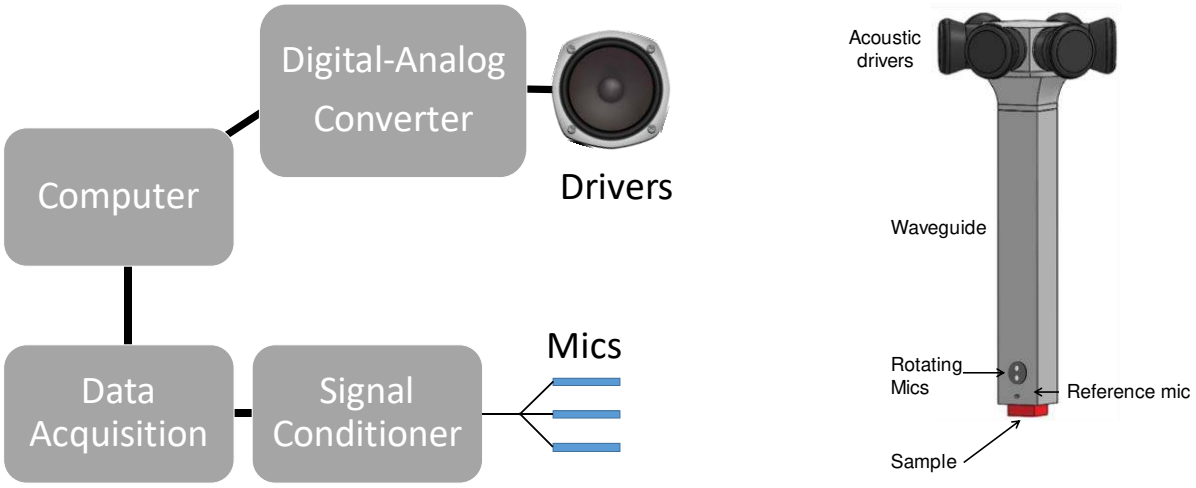

Fig. 3 NIT general arrangement.

D. Grazing Flow Impedance Tube (GFIT)

The NASA Langley GFIT facility is routinely used to determine the acoustic characteristics of noise reduction treatments (acoustic liners) for aircraft jet engine nacelles and nozzles. The facility is a wind tunnel with a 50.8 mm by 63.5 mm rectangular cross section. The flow path (Fig. 4) consists of a straight duct with an upstream acoustic source section using 12 drivers, interchangeable lengths of blank duct, a test section where the liner sample is held along the upper wall of the duct and an array of 95 measurement microphones leading to a 6-driver downstream source section (not used in the current study). Near-anechoic terminating diffusers are employed at each end of the duct to control reflections and reduce overall flow noise. The source sections can generate sound pressure levels up to 150 dB for the frequency range between 400 and 3000 Hz. For flow, pressurized, heated air is supplied to the entrance of the GFIT while a vacuum system is used at the duct exit to 'pull' the flow out of the tube. The static pressure at the test section can thus be held to be near ambient at all flow velocities while also creating an adiabatic wall condition. Grazing flow velocities from 0 to Mach 0.6 are available with such an arrangement.

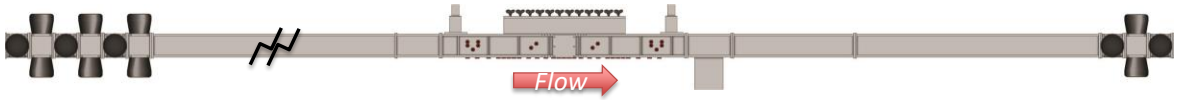

Fig. 4 Sketch of the NASA Langley Grazing Flow Impedance Tube (GFIT).

For the current investigation, the GFIT was operated at Mach 0.0 for all tests. In this 'no-flow' condition, the educed impedances should be similar to the values measured in the NIT.

E. Measurement Process - Stepped-Sine

1. NIT

Tonal acoustic excitation was used at Mach 0.0 for frequencies between 400 and 3000 Hz in 100 Hz increments at *target* sound pressure levels (SPL) of 120 and 140 dB (re: 20 μPa, +/- 0.5 dB). For the NIT, the reference microphone is used to provide feedback for setting the SPL in the waveguide. The amplitude of the acoustic signal is varied until the desired level is achieved. Data from the two rotating plug microphones in the NIT are used to compute the SPL and relative phase for each acoustic test point. The implementation of the switching TMM requires measurements with the microphones in each of the microphone mounting locations for all frequencies. Even with automated switching and level setting, the process can be time consuming requiring approximately one minute per frequency evaluated.

2. GFIT

Like the NIT, stepped-sine excitation was used to create the acoustic source at Mach 0.0 for frequencies between 400 and 3000 Hz in 200 Hz increments at *target* sound pressure levels of 120 and 140 dB. Previous experiments in the GFIT have used a single, fixed reference microphone upstream of the liner to provide feedback for setting the

sound pressure level. This choice led to frequency-dependent variations in level at the liner leading edge as the acoustic standing wave shifts relative to that microphone. An alternative strategy is now employed whereby the group of microphones located +/-76.2 mm from the liner leading edge are surveyed for the maximum SPL value within the group. This value is used as feedback for setting the SPL and seems to provide a more consistent level at the liner leading edge across the frequency range. Data from the 95-microphone array are used to compute the SPL and relative phase at each measurement location.

F. Measurement Process - Swept-Sine

1. NIT

Swept-sine acoustic excitation was used at Mach 0.0 for frequencies between 400 and 3000 Hz at *target* SPLs of 120 and 140 dB (re: 20 μPa). A linear sweep of constant amplitude with a duration of 50 seconds is played through the driver array while recording the response from the reference microphone. The method discussed in Section II.E is used to determine the proper amplitude variation at each frequency to achieve the desired SPL. Multiple iterations of sweep modification can be used if the desired levels are not produced. An example of this process is shown in Fig. 5 where the measured SPL from the NIT reference microphone is plotted versus frequency for four iterations of sweep modification when targeting 140dB.

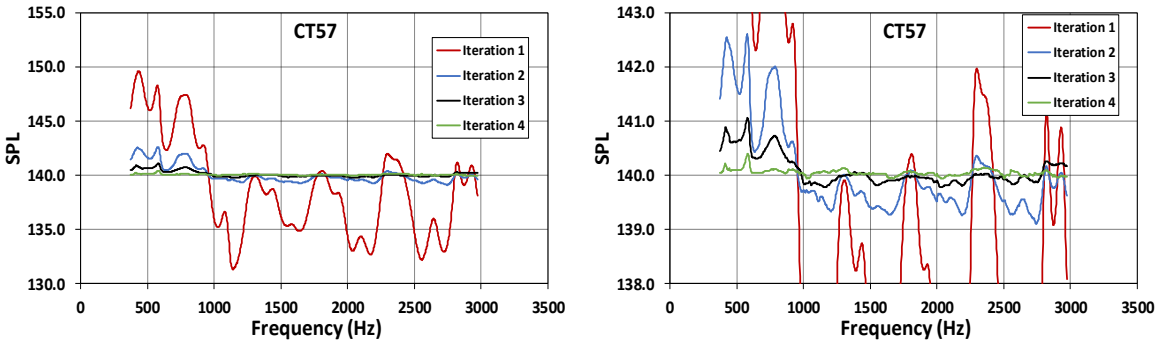

Fig. 5 NIT swept-sine SPL normalization, CT57, 140dB target SPL.

The first iteration at a constant excitation voltage exhibits significant deviation from the target SPL for many frequencies (left chart). A second iteration reduces variation to within 1dB of the target over all the spectrum above 1000 Hz, but amplitudes below that frequency are still higher than desired. The right chart narrows the y-axis scale to show continuing improvement with successive iterations until the target level is achieved for the entire spectrum. Once a satisfactory sweep is created, the signal is sent through the driver array while the microphone responses are recorded. As with the TMM, the microphone locations are then switched and the normalized sweep is played again while recording acoustic data. The time signals are analyzed to compute the SPL and relative phase at each location for all frequencies using the order analysis process presented earlier. Frequency resolution of this process is dependent on the number of spectral lines desired. The current study uses 512 lines to give a resolution of nominally 5 Hz, which required approximately six minutes to acquire in the NIT. Thus, one can acquire very narrowband data significantly faster than with the Stepped-Sine method.

2. GFIT

The method of swept-sine acquisition in the GFIT is very similar to the NIT. However, since the GFIT employs a fixed array of microphones, the final sweep only needs playback once rather than the two times required for the NIT. Also, unlike the Stepped-Sine method, a single microphone located at the leading edge of the liner is used for feedback during the level setting process. Sweep convergence times are similar to the NIT with five to six iterations typically required to normalize the signal to the tolerance band. Implementing the multimicrophone scheme used for the Stepped-Sine method may be developed as a future improvement. The total test times between the two rigs are very similar, taking approximately six minutes to acquire data at 512 frequencies. The savings realized by only playing the final sweep once in the GFIT are offset by the increase in processing time for the greater number of microphones.

G. Impedance Eduction

Regardless of the source of acoustic excitation, the acoustic impedance is educed in the NIT using the Multipoint Method for discrete frequencies as described by Jones and Steide from Ref. 4. For the GFIT, acoustic measurements allow for calculation of liner impedances using these data and the Straightforward Method of Watson [14].

IV. Results and Discussion

A. Liner Impedance Comparison-NIT

Educed impedances calculated from the Stepped-Sine data are presented in Fig. 6 at the two sound pressure levels (120 and 140 dB) tested. For CT57, the resistance and reactance spectra follow expected behavior with very little variation between the two SPLs. Resistance remains fairly flat at around 0.5 up to 2000 Hz where the values begin to increase as antiresonance is approached. Reactance follows a typical *-cot(kd)* pattern with a downward break at 2800 Hz again signaling the approach of antiresonance. Configuration CSQ3 was also designed to be linear with SPL and the impedance spectra show this to be the case. Very little difference is seen in impedance between 120 and 140 dB although minor variations are observed in the resistance at 2200 and 2400 Hz, the frequencies closest to peak anti-resonance. In contrast, the conventional GE01 liner does exhibit some nonlinearity over a significant portion of the frequency range. Resistance more than doubles in the midfrequencies between 800 and 2200 Hz while reactance decreases slightly over the same range. Similar behavior is observed for GE03 but to a lesser degree for the resistance.

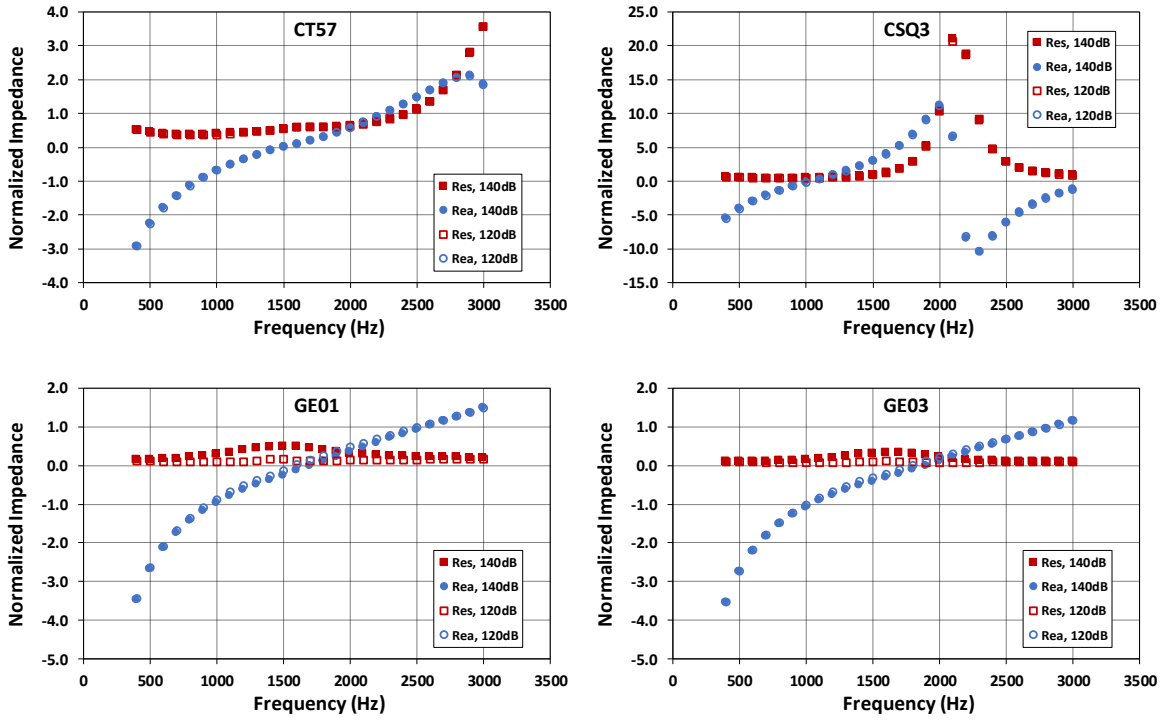

Fig. 6 Normalized impedance, all liners, 120 and 140 dB, Stepped-Sine excitation.

Focusing on the 140 dB results, corresponding SSM data is overlaid with the Stepped-Sine results in Fig. 7. The comparison for liners CT57 and CSQ3 is exceptional with a near-perfect match between methods. The SSM data even correlate well through antiresonance, which is where one could expect differences due to the steep gradients of the spectra. The conventional GE01 and GE03 liners show excellent agreement between the two acquisition methods as well, matching both the resistance and reactance values across the frequency range. Such agreement confirms that the Vold-Kalman filter is providing accurate estimates of acoustic pressure and phase when using sweep excitation.

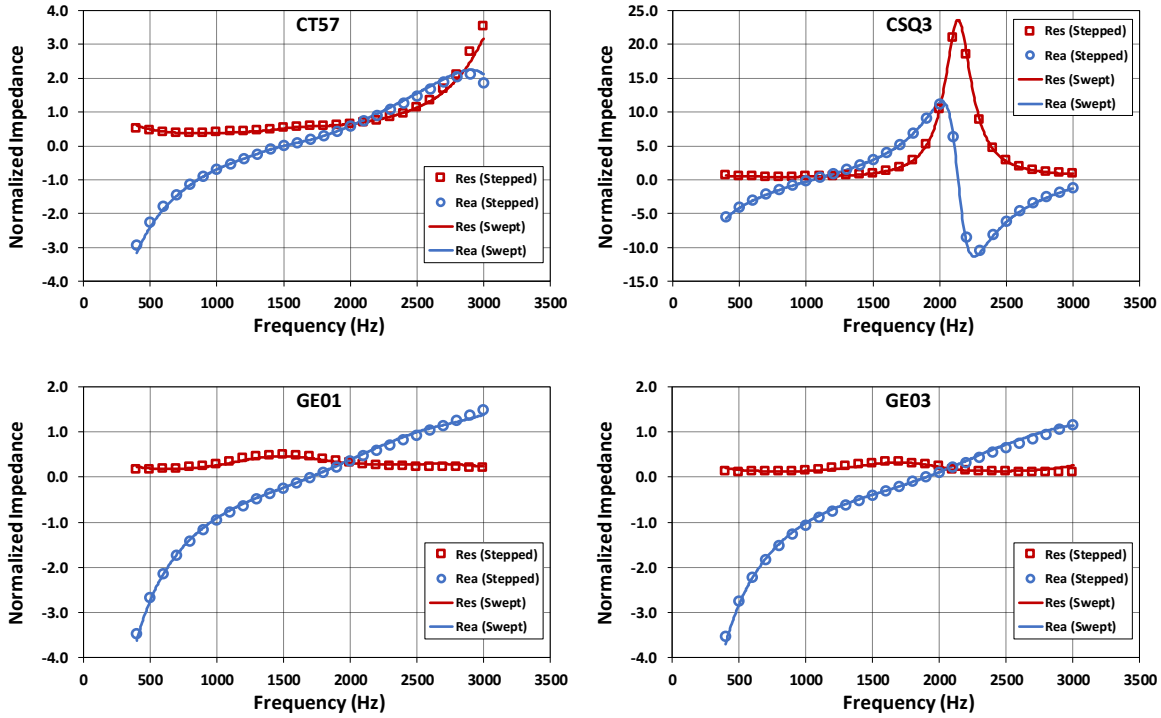

Fig. 7 Educed impedance comparison (Stepped vs. Swept), all liners, 140 dB.

B. Liner Impedance Comparison-GFIT

Data from the GFIT acoustic acquisition are used to educe normal incidence impedance spectra for each liner configuration at 120 and 140 dB for stepped-sine source excitation. The results are shown in Fig. 8. For all cases, variation of the spectra with sound pressure level is minimal. CT57 resonates at 1000 Hz, which is appropriate given the sample depth and puts antiresonance at 2000 Hz. Resistance is approximately 0.5 for frequencies below 1200 Hz. The resistance is noticeably increased for frequencies near antiresonance, which occurs near 2000 Hz, and is reduced to approximately 0.8 at the upper frequencies. With an equivalent chamber depth, CSQ3 behaves similarly to CT57 although the educed reactance gradients are steeper. The conventional liner configurations, GE01 and GE03, exhibit relatively flat resistance spectra with little variation as SPL increases. Reactance follows a $-cot(kd)$ pattern with a slightly steeper slope for GE01 as compared to GE03.

Notably absent in the data from the GE01 and GE03 configurations is the midfrequency rise in resistance observed with the NIT results (especially for 140 dB). These frequencies correspond with where the liner has a significant attenuation effect in the GFIT thus rapidly reducing the SPL incident on the surface of the liner as one moves axially along its length. Therefore, while the portion of the liner may experience levels sufficient enough to cause nonlinear behavior, the majority of the liner is not which results in the spectra shown.

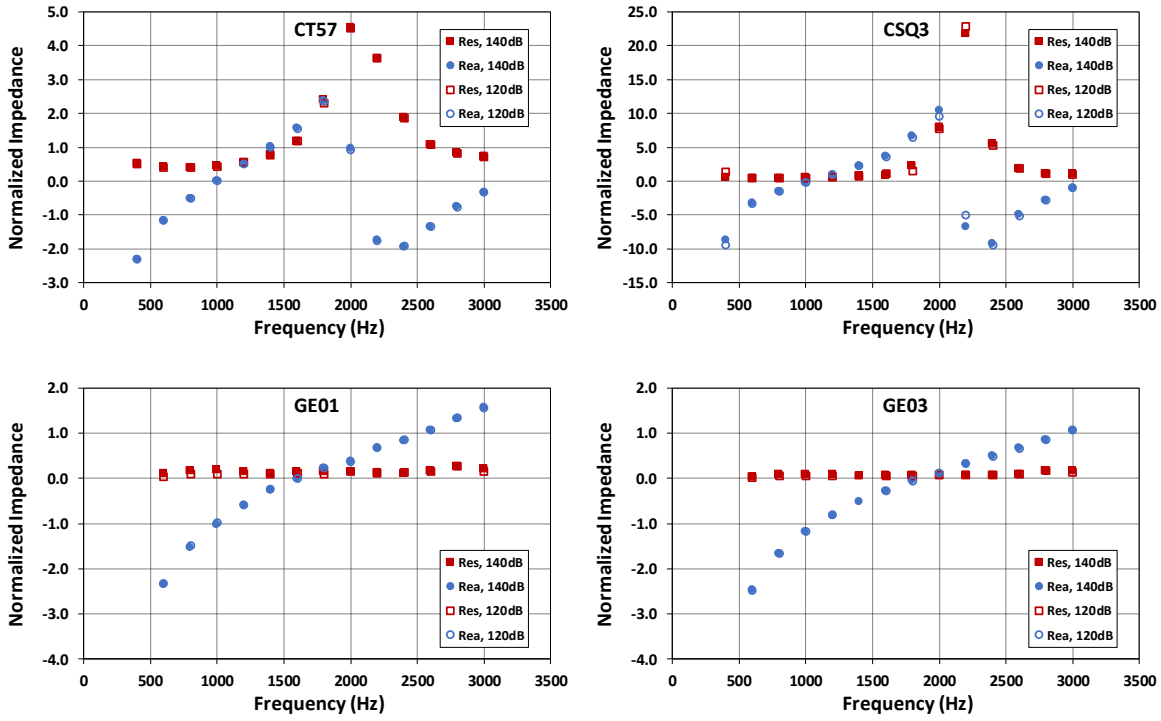

Fig. 8 Normalized impedance, all liners, 120 and 140 dB, stepped-sine excitation.

The use of the Swept-Sine Method in the GFIT produces some interesting results for these liner configurations. Figure 9 shows the educed normalized impedance spectra for 140dB excitation for all four samples. While the overall

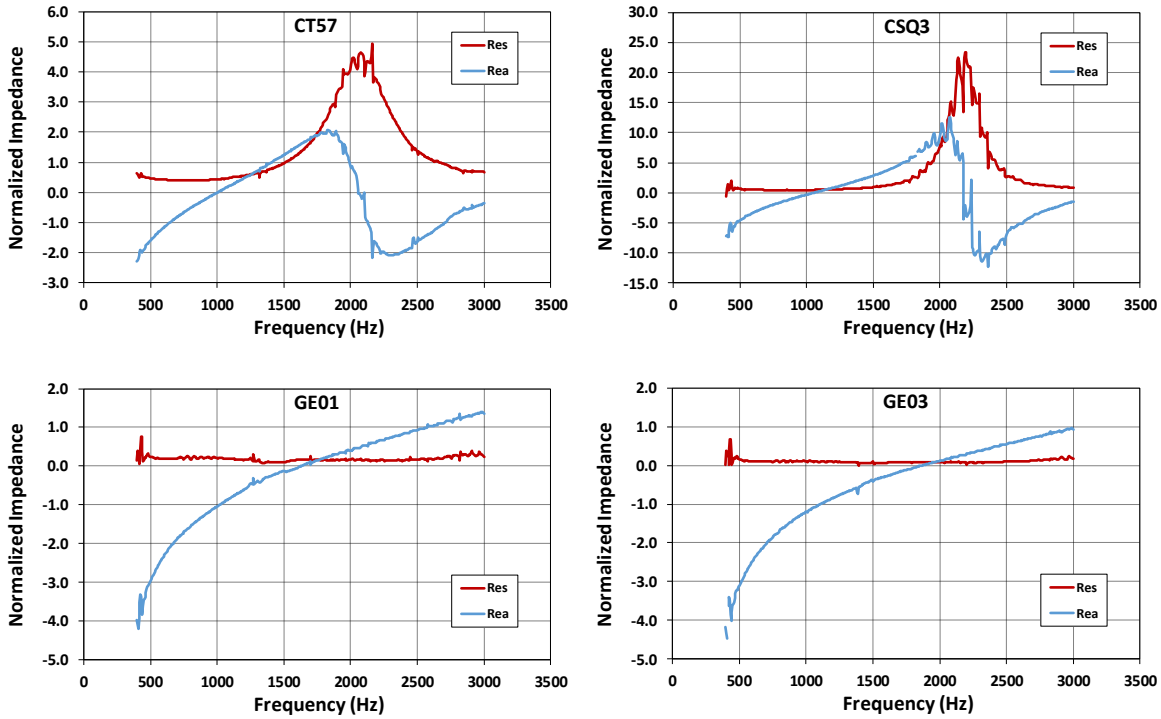

Fig. 9 Normalized impedance, all liners, 140 dB, swept-sine excitation.

shape of the spectra match the previously shown Stepped-Sine data, the curves do not exhibit the smoothness observed in the NIT data. It had been expected that educed impedance spectra would be nearly as smooth as those attained with the NIT data. However, results from GE01 and GE03 show some scatter at the lowest frequencies and some ripple at other frequency bands. These features do not readily correlate to some property of the liner. Spectra from data collected with the CT57 and CSQ3 samples show significant impedance fluctuations near antiresonance. Such results, though, are generally of lesser interest as they correspond to conditions where the liner is ineffective for noise reduction. The Straightforward Method of eduction, like other eduction schemes, has been shown to provide spurious answers at these conditions. Further work is planned to determine if a lengthening of the sweep is required to improve averaging at each frequency or if the indirect CHE method of Watson [14] is better able to educe the impedance under those conditions.

Figure 10 is a plot of the comparison of impedance results of all liner configurations for stepped-sine and swept-sine source excitation. One can see good agreement between the two datasets over the full frequency range even with the aforementioned issues near antiresonance. Acquisition time for the SSM data averaged nine minutes per configuration (it took 15 minutes to measure the lower-resolution Stepped-Sine data) with no loss of accuracy.

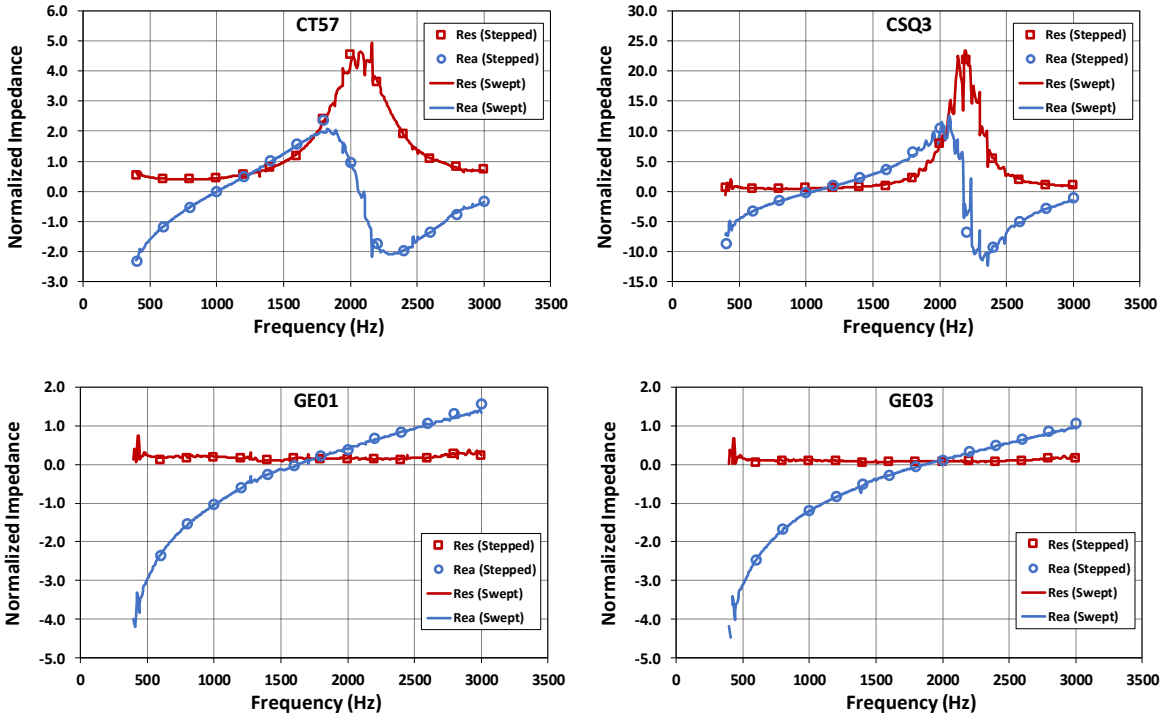

Fig. 10 Educed impedance comparison (Stepped vs. Swept), 140 dB.

V. Concluding Remarks

From the testing and analysis performed using the NIT and GFIT, some conclusions can be made regarding the efficiency and accuracy of the Swept-Sine Method (SSM) relative to the Stepped-Sine Method (StepSM).

1. Application of the Vold-Kalman order tracking filter allows for the use of swept-sine acoustic excitation to acquire the necessary amplitude and phase information for impedance eduction.

2. Automatic source amplitude normalization achieves a nearly flat excitation spectrum over the desired frequency range.

3. Impedances calculated from NIT SSM data, using the Switching Two-Microphone Method and multipoint analysis, match very well to those determined from the previously used StepSM.

4. Impedances calculated from GFIT SSM data, using the Straightforward Method of impedance eduction, match the StepSM results well but exhibit significant variation near antiresonance when liner attenuation is low. Further study is warranted to isolate the cause(s) and reduce variability in what should be smooth, continuous impedance spectra.

5. Using SSM provides significantly higher frequency resolution *while reducing* total acquisition time relative to even a sparse frequency Stepped-Sine dataset. Typical test time reductions of 70% in the NIT and 40% in the GFIT were observed.

Extension of this method is underway to include flow effects in the GFIT where the accompanying broadband noise must be filtered out. Further work to determine the optimum sweep length, acoustic driver phasing to maximize excitation levels, and improve convergence times of the normalized sweep signal is planned. The intent is to supplant much of Stepped-Sine testing with SSM for production and research work in these test rigs.

Acknowledgments

The authors would like to thank Alonzo 'Max' Reid of Science and Technology Corporation for his efforts in collecting the experimental data. Funding for this effort was provided under the NASA Advanced Air Transport Technology Project for the Advanced Air Vehicles Program.

References

[1] Dickens, Paul., Smith, John, and Wolfe, Joe., "Improved Precision in Measurements of Acoustic Impedance Spectra Using Resonance-free Calibration Loads and Controlled Error Distribution," *Journal of the Acoustical Sociey of America*, Vol. 121, No. 3, pp. 1471-1481, May 2007.

[2] Dean, P. D., "An *In Situ* Method of Wall Acoustic Impedance Measurement in Flow Ducts," *Journal of Sound and Vibration*, Vol. 34, No. 1, pp. 97-130, Jan 1974.

[3] Gaeta, R. J., Mendoza, J. M., and Jones, M. G., "Implementation of In-Situ Impedance Techniques on a Full Scale Aero-Engine System," AIAA Paper 2007-3441, 13th AIAA/CEAS Aeroacoustics Conference, May 2007.

[4] Jones, Michael G., and Stiede, Patricia E., "Comparison of Methods for Determining Specific Acoustic Impedance," *Journal of the Acoustical Sociey of America*, Vol. 101, No. 5, Pt. 1, pp. 2694-2704, May 1997.

[5] Jones, M. G., Nark, D. M., Baca, A., and Smith, C. R., "Applications of Parallel-Element, Embedded Mesh-Cap Acoustic Liner Concepts," AIAA Paper 2018-3445, 24th AIAA/CEAS Aeroacoustics Conference, June 2018.

[6] Jones, M. G., Howerton, B. M., and Ayle, E., "Evaluation of Parallel-Element, Variable-Impedance Broadband Acoustic Liner Concepts," AIAA Paper 2012-2194, 18th AIAA/CEAS Aeroacoustics Conference, June 2012.

[7] Bodén, H., "The Effect of High Level Multi-tone Excitation on the Acoustic Properties of Perforates and Liner Samples," AIAA Paper 2012-2151, 18th AIAA/CEAS Aeroacoustics Conference, June 2012.

[8] Bodén, H., "Acoustic Properties of Perforates Under High Level Multi-tone Excitation," AIAA Paper 2013-2175, 19th AIAA/CEAS Aeroacoustics Conference, May 2013.

[9] H. Wold, "A Study in the Analysis of Stationary Time Series," Ph.D. Dissertation, Stockholm, Sweden, 1938.

[10] H. Vold, B. Schwarz, and M. Richardson, "Measuring Operating Deflection Shapes Under Non. Stationary Conditions," *Proceedings of International Modal Analysis Conference XVIII*, San Antonio, TX, February 2000.

[11] Vold, H., and J. Leuridan. "High Resolution Order Tracking at Extreme Slew Rates, Using Kalman Tracking Filters." SAE Technical Paper No. 931288. 1993.

[12] R. E. Kálmán, "A New Approach to Linear Filtering and Prediction Problems," *ASME Journal of Basic Engineering*, Vol. 82 (Series D), March 1960, pp. 35–45.

[13] Tuma, J., "Setting the passband width in the Vold-Kalman order tracking filter," *12th International Congress on Sound and Vibration*, (ICSV12), Lisboa, Portugal, July 2005.

[14] Watson, W. R., and Jones, M. G., "A Comparative Study of Four Impedance Eduction Methodologies Using Several Test Liners," AIAA Paper 2013-2274, 19th AIAA/CEAS Aeroacoustics Conference, May 2013.